JOURNAL OF PROPULSION AND POWER
Vol. 18, No. 3, May–June 2002

Ejector Primary Flow Molecular Weight Effects in an Ejector–Ram Rocket Engine

Sam Han,* John Peddieson, Jr.,† and David Gregory‡
Tennessee Technological University, Cookeville, Tennessee 38505

The effects of primary flow molecular weight on the ejector performance in a generic rocket-based combined-cycle engine are examined by using steady-state, one-dimensional compressible flow equations. Ejector performance in terms of specific impulse, bypass ratio, thrust, and thrust augmentation factor are presented for three primary fluids with molecular weights of 2, 18, and 29, covering a range of primary rocket stagnation conditions, ejector geometries, and freestream conditions.

Nomenclature

A	=	area, m^2
C_v, C_p	=	specific heat at constant volume, pressure, J/kg · K
I_{sp}	=	specific impulse, s
M	=	Mach number
M_w	=	molecular weight
$\dot{m}$	=	mass flow rate, kg/s
$\dot{n}$	=	mole flow rate, mole/s
P	=	static pressure, Pa
$\dot{q}$	=	combustion energy generation rate, W
R	=	gas constant, J/kg · K
T	=	temperature or thrust, K or N
u	=	velocity, m/s
α	=	bypass ratio
γ	=	specific heat ratio
ρ	=	density, kg/m^3
ϕ	=	thrust augmentation factor

Subscripts

e	=	exit of the mixing region
ejector	=	ejector mode
i	=	inlet of the mixing region
p	=	primary flow
rocket	=	rocket-only mode
s	=	secondary flow
t	=	stagnation condition
0	=	freestream condition
10	=	nozzle exit

Superscripts

$*$	=	primary rocket throat
$-$	=	molar property

Introduction

TO increase the payload and improve the reliability of the Earth-to-orbit (ETO) reusable launch vehicles (RLV), rocket-based combined-cycle (RBCC) engines are currently under development.[1] In one of the RBCC engine concepts, a rocket is used as an ejector during the initial acceleration ($M_0 < 3.0$) and as a conventional rocket when $M_0 > 6.0$. This concept is called the ejector–ram rocket engine and is the simplest RBCC engine configuration.[2,3]

Ejectors have been used in many industrial applications, such as in pumping,[4] chemical lasers,[5,6] and airbreathing jet engine development.[7,8] Optimization of ejector performance depends on the particular application. It is used to maximize the entrainment ratio in pumping, to increase the pressure recovery in the chemical laser, and to augment thrust in aerospace applications. Ejectors used in RBCC engines are similar to those used in ramjet engines in aerospace applications.

Ejector efficiency is often measured by the ability of the primary flow to entrain the secondary flow. In aircraft and RBCC applications, atmospheric air is the secondary fluid. The primary fluid can be air or any other fluid with different thermodynamic properties. Numerous studies have shown that the ejector performance depends strongly on the properties of the primary fluid, in particular its molecular weight.[9,10]

The present study seeks to evaluate the effects of molecular weight of several primary fluids on the ejector efficiency of a generic RBCC engine. Such results for the ejector–ram rocket operation covering the flight regime of $M_0 = 0 \sim 3.0$ are not currently available in the literature.

Method of Analysis

Assumptions

Figure 1 shows the schematic view of a generic ejector–ram rocket engine. The engine has four components: an inlet, a mixing region of constant cross-sectional area A, a combustor, and an exit nozzle. Actual physical processes in these engine components are very complex and need detailed experimental and numerical analysis as discussed in various hypersonic airbreathing engine studies.[11] One of the simplest methods currently used is to employ the steady-state control volume concept. This method provides an idealized and yet simple closed-form solution for a quick parametric study of various operating conditions.

The ejector primary fluid is assumed to be an ideal gas with known stagnation pressure and stagnation temperature. The primary flow is choked at the rocket throat A_p^* and then expands supersonically entraining the secondary fluid (atmospheric air) by suction and viscous interaction. The inlet region exit plane is located where the static pressures of both fluids are in equilibrium ($p_{pi} = p_{si} = p_i$).

When the static pressure p_i and an isentropic compression of the ingested secondary flow are assumed, conditions of the secondary flow at the inlet of the mixing region (or at the end of inlet region) are found. Likewise, an isentropic expansion of the primary flow from the rocket stagnation pressure p_{tp} to the static pressure p_i gives the primary flow conditions at the inlet of the mixing region.

Received 12 March 2001; revision received 12 September 2001; accepted for publication 23 October 2001.

*Professor, Department of Mechanical Engineering, P.O. Box 5014; shan@tntech.edu. Member AIAA.
†Professor, Department of Mechanical Engineering.
‡Graduate Student, Department of Mechanical Engineering.

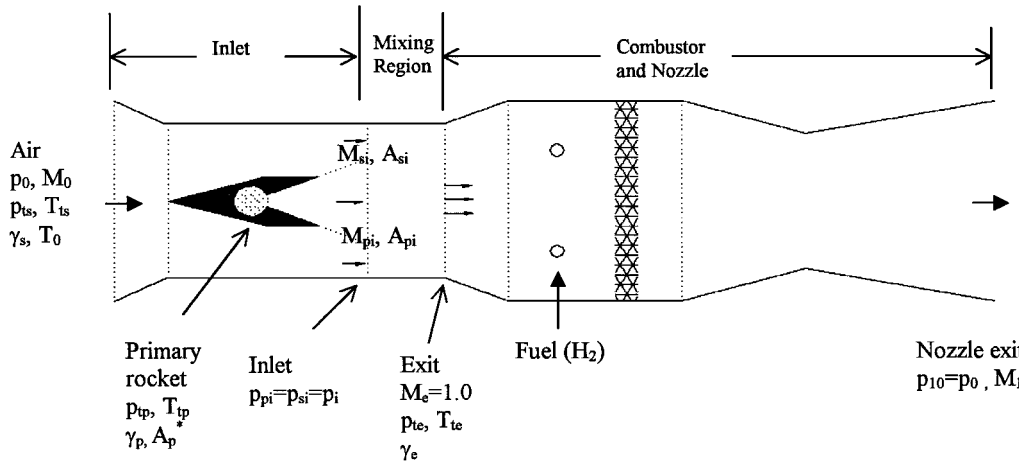

Fig. 1 Schematic view of an ideal ejector–ram rocket engine.

The unknown inlet pressure p_i is determined by considering the mass, linear momentum, and energy balances for the control volume surrounding the mixing region with known exit conditions. In a real ejector–ramjet operation, the supersonic primary flow interacting with the subsonic secondary flow generates a series of oblique[12] and/or a normal shock[13] so that the resulting mixture leaves the mixing region as a supersonic or a subsonic flow. To simplify the analysis, however, it is assumed that there are no shocks, and the flow is allowed to accelerate until it is choked at the end of mixing region (downstream choking). This is the assumption used in Ref. 11 and is adopted in the present analysis. Note that no assumptions are made for the inlet Mach numbers of both the primary and the secondary flows. The present approach is different from other studies in which the secondary flow is choked at the inlet (upstream choking), whereas the downstream Mach number is subsonic.[14]

The purpose of the ejector is to increase the flow rate through the engine and use the oxygen in the air as the oxidizer for the fuel injected in the combustor. When the conservation principles are applied to the control volume surrounding the combustion chamber and the exit nozzle, the thrust of the engine is calculated. The heated gas mixture is assumed to expand ideally to the atmospheric pressure at the exit of the nozzle without frictional loss.

Equations

With the assumptions made for the inlet, the unknown inlet static pressure and the secondary flow inlet Mach number are related by

$$M_{\mathrm{si}} = \left\{ \frac{2}{\gamma_s - 1} \left[\left(\frac{p_{\mathrm{ts}}}{p_0} \frac{p_0}{p_i} \right)^{(\gamma_s - 1)/\gamma_s} - 1 \right] \right\}^{0.5} \tag{1}$$

where p_{ts}/p_0 is the known atmospheric flight condition. Likewise, inlet static pressure and inlet primary flow Mach number are related by

$$M_{\mathrm{pi}} = \left\{ \frac{2}{\gamma_p - 1} \left[\left(\frac{p_{\mathrm{tp}}}{p_0} \frac{p_0}{p_i} \right)^{(\gamma_p - 1)/\gamma_p} - 1 \right] \right\}^{0.5} \tag{2}$$

where the primary rocket stagnation pressure ratio p_{tp}/p_0 is known.

For the isentropic expansion of the primary flow, the ratio of A_{pi} to A_p^* is

$$\frac{A_{\mathrm{pi}}}{A_p^*} = \left\{ \frac{1}{M_{\mathrm{pi}}^2} \left[\frac{2}{\gamma_p + 1} \left(1 + \frac{\gamma_p - 1}{2} M_{\mathrm{pi}}^2 \right) \right]^{(\gamma_p + 1)/(\gamma_p - 1)} \right\}^{0.5} \tag{3}$$

Thus, the area ratio for the primary flow at the inlet of the mixing region is

$$A_{\mathrm{pi}}/A = \left(A_{\mathrm{pi}}/A_p^*\right)\left(A_p^*/A\right) \tag{4}$$

and the area ratio for the secondary flow at the inlet is

$$A_{\mathrm{si}}/A = 1 - A_{\mathrm{pi}}/A \tag{5}$$

Mass flow rate of the secondary flow per unit area of the ejector is

$$\frac{\dot{m}_s}{A} = \sqrt{\frac{\gamma_s}{R_s T_{\mathrm{ts}}}} P_{\mathrm{ts}} M_{\mathrm{si}} \frac{A_{\mathrm{si}}}{A} \left(1 + \frac{\gamma_s - 1}{2} M_{\mathrm{si}}^2 \right)^{-[(\gamma_s + 1)/2(\gamma_s - 1)]} \tag{6}$$

and for the primary flow,

$$\frac{\dot{m}_p}{A} = \sqrt{\frac{\gamma_p}{R_p T_{\mathrm{tp}}}} P_{\mathrm{tp}} M_{\mathrm{pi}} \frac{A_{\mathrm{pi}}}{A} \left(1 + \frac{\gamma_p - 1}{2} M_{\mathrm{pi}}^2 \right)^{-[(\gamma_p + 1)/2(\gamma_p - 1)]} \tag{7}$$

One measure of ejector efficiency is the bypass ratio, defined by

$$\alpha = \dot{m}_s/\dot{m}_p \tag{8}$$

All flow quantities discussed so far can be determined if the inlet pressure p_i of the mixing region is known. To determine this, conservation equations for the mixing region are used. The mass conservation is expressed as

$$\dot{m}_s + \dot{m}_p = \dot{m}_e \tag{9}$$

and the energy equation shows that

$$\frac{T_{\mathrm{te}}}{T_{\mathrm{tp}}} = \frac{C_{pp}}{(\alpha + 1) C_{pe}} \left[\alpha \frac{C_{ps}}{C_{pp}} \frac{T_{\mathrm{ts}}}{T_{\mathrm{tp}}} + 1 \right] \tag{10}$$

Because the flow at the exit is choked, the temperature at the exit is related to the corresponding stagnation temperature by

$$T_e/T_{\mathrm{te}} = 2/(\gamma_e + 1) \tag{11}$$

Combining Eqs. (10) and (11) yields

$$\frac{T_e}{T_{\mathrm{tp}}} = \left(\frac{2}{\gamma_e + 1} \right) \frac{C_{pp}}{(\alpha + 1) C_{pe}} \left[\alpha \frac{C_{ps}}{C_{pe}} \frac{T_{\mathrm{ts}}}{T_0} \frac{T_0}{T_{\mathrm{tp}}} + 1 \right] \tag{12}$$

The exit static pressure of the mixture is

$$p_e = \rho_e R_e T_e \tag{13}$$

where the density of the mixture with $M_e = 1$ is

$$\rho_e = \frac{\dot{m}_p (1 + \alpha)}{A \sqrt{\gamma_e R_e T_e}} \tag{14}$$

By the use of Eq. (7), the mass flow rate of the primary flow at the throat is (A_p^*, $M_p^* = 1$),

$$\frac{\dot{m}_p}{A} = \sqrt{\frac{\gamma_p}{R_p T_{tp}}} P_{tp} \frac{A_p^*}{A} \left(\frac{\gamma_p + 1}{2} \right)^{-[(\gamma_p + 1)/2(\gamma_p - 1)]} \tag{15}$$

When Eqs. (13–15) are combined and divided by the atmospheric pressure, p_0 leads to

$$\frac{p_e}{p_0} = \sqrt{\frac{\gamma_p R_e}{\gamma_e R_p}} \frac{A_p^*}{A} (1 + \alpha) \frac{p_{tp}}{p_0} \sqrt{\frac{T_e}{T_{tp}}} \left(\frac{\gamma_p + 1}{2} \right)^{-[(\gamma_p + 1)/2(\gamma_p - 1)]} \tag{16}$$

Next, the momentum balance for the mixing region, neglecting the frictional losses, is

$$(p_i - p_e)A = -u_s \dot{m}_s - u_p \dot{m}_p + u_e \dot{m}_e \tag{17}$$

By the use of the ideal gas equation and the definition of Mach number, it can be shown that $\dot{m}u = M^2 pA\gamma$. Thus, Eq. (17) can be rewritten in the following form:

$$\frac{p_i}{p_0} = \frac{p_e}{p_0} (1 + \gamma_e) \left(1 + \frac{A_{si}}{A} \gamma_s M_{si}^2 + \frac{A_{pi}}{A} \gamma_p M_{pi}^2 \right)^{-1} \tag{18}$$

where p_e/p_0 is given by Eq. (16).

The foregoing analysis is similar to the method described in Ref. 11, except that dissimilar fluid effects are included herein. The thermodynamic properties of mixture are found by using the calculated primary and secondary mass flow rates. The molecular weight of the mixture is

$$M_{w_e} = y_s M_{w_s} + y_p M_{w_p} \tag{19}$$

where the mole fractions of the primary and secondary flows are

$$y_p = \dot{n}_p/(\dot{n}_p + \dot{n}_s), \qquad y_s = \dot{n}_s/(\dot{n}_p + \dot{n}_s) \tag{20}$$

Other thermodynamic properties of the mixture are

$$R_e = \bar{R}_{univ} \big/ M_{w_e}, \qquad C_{p_e} = \left(y_s \bar{C}_{p_s} + y_p \bar{C}_{p_p} \right) \big/ M_{w_e}$$

$$\gamma_e = C_{p_e} \big/ C_{v_e} \tag{21}$$

The static pressure at the nozzle exit is assumed to be atmospheric pressure. Other properties at the nozzle exit are found by using conservation laws for the control volume surrounding the combustor and the exit nozzle. Mass conservation requires that

$$\dot{m}_s + \dot{m}_p + \dot{m}_{H_2} = \dot{m}_{10} \tag{22}$$

where $\dot{m}_{H_2}$ is the fuel flow rate and the subscript 10 represents the nozzle exit plane consistent with Ref. 11. When a 100% reaction with the oxygen contained in the secondary flow (air) is assumed,

$$\dot{m}_{H_2} = 0.029 \dot{m}_s \tag{23}$$

The hydrogen mass entering the combustion chamber is relatively small and is, therefore, neglected in the mass and momentum balance equations. However, the energy released from combustion is added in the energy equation. It is assumed that a primary flow, other than hydrogen, does not contain any unburned fuel. For the hydrogen primary flow, a small fraction of primary flow reacts with the oxygen in the secondary flow, and no fuel injection is needed in the combustion chamber. As an approximation, it is assumed that the heating value of water vapor at 1500 K is about 9.15×10^7 J/kg of hydrogen. The energy release from combustion with an equivalence ratio of 0.33 is

$$\dot{q} = 8.75 \times 10^5 \dot{m}_s \tag{24}$$

It is assumed that energy added to the mixed flow in the combustor increases the stagnation temperature but not the stagnation pressure. The expansion through the nozzle is assumed to be isentropic with $\gamma_{10} = \lambda_e$ and $p_{10} = p_0$. Thus,

$$M_{10} = \left\{ [2/(\gamma_e - 1)] \left[(p_{te}/p_0)^{(\gamma_e - 1)/\gamma_e} - 1 \right] \right\}^{0.5} \tag{25}$$

The stagnation temperature at the exit of the nozzle is equal to the stagnation temperature at the end of combustor,

$$T_{t10} = T_{te} + \dot{q} \big/ C_{p_e} \dot{m}_e \tag{26}$$

Calculation Procedures

The following trial and error method is used to solve the preceding set of equations:

1) Assume an inlet pressure ratio, $(P_0/P_i)_{old}$.

2) Calculate M_{pi} and the area ratio A_{si}/A using Eqs. (2–5). If the area ratio is less than zero, no solution is possible and calculation stops. If not, go to step 3.

3) Calculate M_{si}, $\dot{m}_p$, $\dot{m}_s$, and α by Eqs. (1) and (6–8). Also evaluate the mixture properties.

4) Calculate T_e/T_{tp} by Eq. (12) and new inlet pressure $(p_0/p_i)_{new}$.

5) Compare the old and new inlet pressures. If they do not match within a prescribed tolerance, the inlet pressure is updated by

$$(p_0/p_i)_{old} = f(p_0/p_i)_{new} + (1 - f)(p_0/p_i)_{old} \tag{27}$$

and the procedure is repeated again from step 2 until a convergence is obtained. For the present analysis, a relative error tolerance of 10^{-3} and a weighting factor $f = 0.05$ are used. The convergence rate depends critically on the initial choice of the pressure ratio in step 1. In the present study, the initial guess of the pressure ratio is prescribed by $p_i/p_0 = 0.95 \min(p_{tp}/p_0, p_{ts}/p_0)$. This is a conservative initial guess, and convergence was obtained for all cases with the number of iterations ranging from few tens to few hundreds.

With the preceding set of procedures, conditions at the inlet of the mixing region are calculated: Mach numbers for both primary and secondary flows, equilibrium static pressure and mass flow rates, and the compression ratio. Thus, two parameters that determine the efficiency of ejector, namely, the bypass ratio and the compression ratio, are determined.

The purpose of an ejector is to increase the engine thrust and its specific impulse. In the context of the present simplified analysis, the thrust per unit area of the ejector mode can be expressed by

$$T_{ejector} = \dot{m}_e u_{10} - \dot{m}_s u_0 \tag{28}$$

The specific impulse is defined by

$$I_{sp} = T_{ejector}/g_0 \dot{m}_p \tag{29}$$

where g_0 is the gravitational acceleration at sea level.

The thrust augmentation factor is defined by the ratio of the thrust obtained by using the primary rocket as an ejector to the thrust obtainable from the primary rocket operating alone without the ejector system. The thrust obtainable from the stand-alone mode is

$$T_{rocket} = \dot{m}_p u_{p0} \tag{30}$$

where u_{p0} is the maximum obtainable primary flow speed at the rocket nozzle exit plane.

Thus, the thrust augmentation factor is defined by

$$\phi = (1 + \alpha)(u_{10}/u_{p0}) - \alpha(u_0/u_{p0}) \tag{31}$$

The freestream velocity appearing in these expressions is

$$u_0 = M_0 \sqrt{\gamma_s R_s T_0} \tag{32}$$

where M_0 is the flight Mach number and T_0 is known atmospheric temperature. The exit velocity of the stand-alone mode is

$$u_{p0} = M_{p0} \sqrt{\gamma_p R_p T_{p0}} \tag{33}$$

Given an isentropic expansion of the primary flow from the stagnation condition to the atmospheric condition, the corresponding exit conditions are

$$M_{p0} = \left\{[2/(\gamma_p - 1)]\left[(p_{\text{tp}}/p_0)^{(\gamma_p - 1)/\gamma_p} - 1\right]\right\}^{0.5} \tag{34}$$

$$T_{p0} = T_{\text{tp}}\left\{1 + [(\gamma_p - 1)/2]M_{p0}^2\right\}^{-1} \tag{35}$$

Likewise, for the ejector operation, the nozzle exit velocity and temperature are

$$u_{10} = M_{10}\sqrt{\gamma_e R_e T_{10}} \tag{36}$$

$$T_{10} = T_{t10}\left\{1 + [(\gamma_e - 1)/2]M_{10}^2\right\}^{-1} \tag{37}$$

where M_{10} and T_{t10} are given by Eqs. (25) and (26), respectively.

Results

There are many variables that control the ejector performance: the molecular weight of the primary flow, the primary rocket stagnation temperature and pressure, the freestream Mach number, the geometry of the ejector, and the specific heat ratios. The molecular weight of the secondary flow is fixed to that of air, but its temperature and pressure are functions of M_0.

The objective herein is to determine the effects of molecular weight of the primary flow on the bypass ratio, thrust augmentation, and specific impulse. Three primary flows with molecular weights of 2 (hydrogen), 18 (water vapor), and 29 (a generic hydrocarbon) are considered. The baseline ejector variables are $p_{\text{tp}}/p_0 = 15$, $T_{\text{tp}}/T_0 = 10$, $A/A_p^* = 12$, and $\gamma_s = \gamma_p = 1.4$. These are selected to correspond to a calculation in Ref. 11 that serves as a reference case in subsequent discussions. Three variables, p_{tp}/p_0, T_{tp}/T_0, and A/A_p^* are selected as variable parameters. The effects of variable γ_p are not considered for simplification.

Effects of Primary Flow Stagnation Pressure

Figure 2 reports results obtained by varying the primary rocket stagnation pressure from 3 to 40 while holding all other baseline ejector variables fixed. The situation simulated is that of the engine starting to accelerate at ground level ($M_0 = 0.01$).

Figure 2a shows dependency of the inlet Mach number for both primary, M_{pi}, and secondary, M_{si}, flow on the stagnation pressure and the molecular weight of the primary flow. The inlet primary flow is supersonic and the inlet secondary flow is subsonic for all pressure ranges and for all molecular weights. The inlet primary Mach number increases as both the molecular weight and the pressure increase. For large molecular weight, increasing primary pressure decreases the secondary flow area until the secondary flow

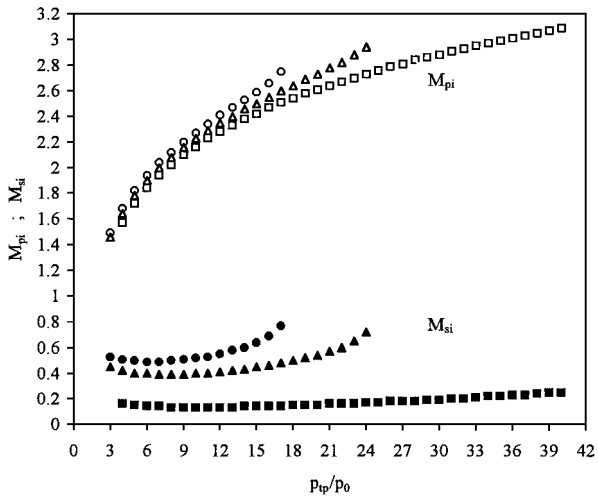

a) Primary and secondary flow inlet Mach numbers

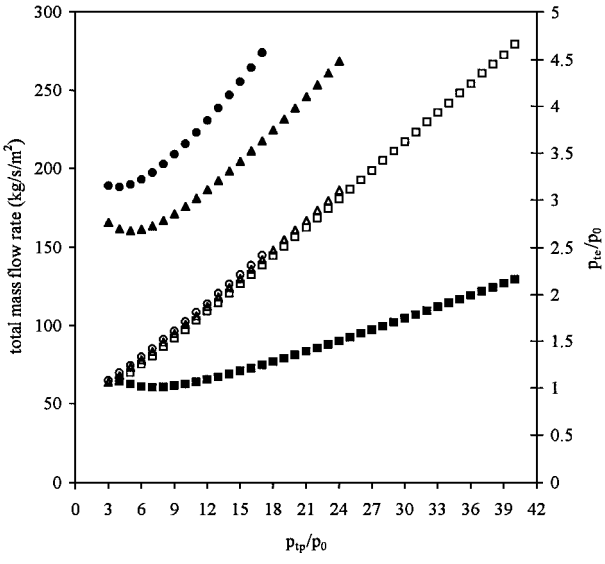

b) Total mass flow rate and the compression ratio

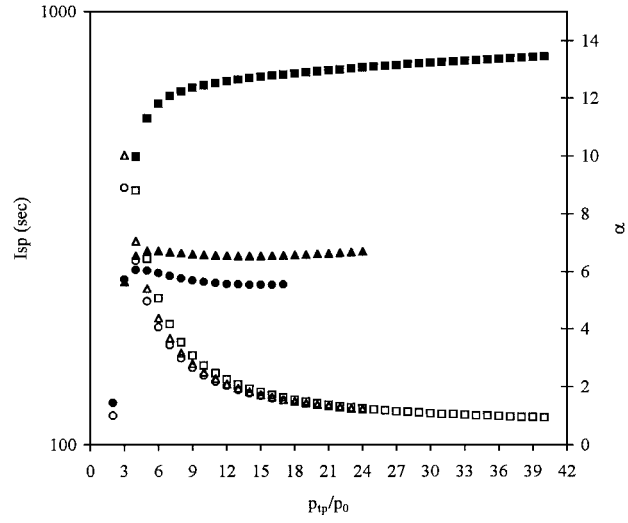

c) Specific impulse and the bypass ratio

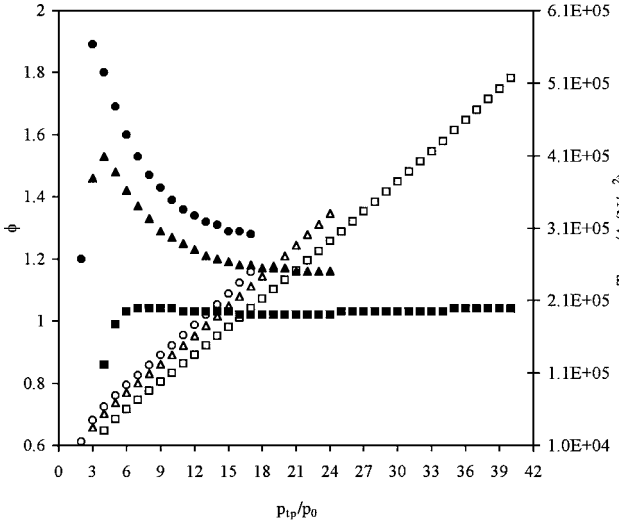

d) Total thrust and the thrust augmentation factor

Fig. 2 Effects of the primary flow stagnation pressure (p_{tp}/p_0) and the molecular weight (M_{w_p}) on the baseline ejector performance at sea level (M_0 = 0.01) with $T_{\text{tp}}/T_0 = 15$ and $A/A_p^* = 12$: $M_{w_p} = 2$ (□), $M_{w_p} = 18$ (△), and $M_{w_p} = 29$ (○). (Unless noted otherwise, open symbols go with the right ordinate and filled symbols with the left ordinate.)

is completely blocked (see discussion hereafter). The secondary flow inlet Mach number increases rapidly during this period. There are allowable pressure limitations for meaningful solutions: a minimum pressure limitation for $M_{w_p} = 2$ and a maximum pressure limitation for $M_{w_p} = 18$ and 29. For $M_{w_p} = 2$, the compression ratio, p_{te}/p_0, becomes less than one when the stagnation pressure is less than four. This is due to an insufficient primary mass flow rate because the density of the choked primary flow is proportional to the molecular weight. For larger molecular weights, on the other hand, expansion of the primary flow is such that the area ratio A_{pi}/A approaches unity and the secondary flow is completely blocked. This occurred at pressure ratios greater than 24 for $M_{w_p} = 18$ and 15 for $M_{w_p} = 29$. To operate at higher primary flow stagnation pressures, A/A_p^* must be increased for the larger molecular weight cases. No maximum pressure limitation was detected for $M_{w_p} = 2$, and, consequently, stagnation pressures much higher than the baseline case can be used for the hydrogen ejector. Of course, these limiting pressure ranges will be different for different combinations of baseline variables.

Figure 2b shows total mass flow rate $\dot{m}_e$ and the compression ratio p_{te}/p_0 as functions of the primary flow stagnation pressure ratio and molecular weight. Total mass flow rate is a strong function of molecular weight. It increases with increasing molecular weight due to higher primary mass flow rate and accompanying secondary mass flow rate. Total mass flow rate decreases initially as the stagnation pressure increases to about 2–6 in spite of increasing primary flow rate. This is due to the secondary mass flow rate rapidly decreasing, as indicated by the decreasing inlet Mach number as shown in Fig. 2a. The secondary mass flow rate increases beyond these pressure ranges and the total mass flow increases as the stagnation pressure increases. The compression ratio increases slightly with increasing molecular weight and it increases almost linearly with increasing stagnation pressure. For $M_{w_p} = 2$, the compression ratio is less than 1.0 when the stagnation pressure is below four, which is the lower pressure limit.

Figure 2c shows the specific impulse and the bypass ratio as functions of the primary rocket stagnation pressure and its molecular weight. As expected, specific impulse decreases with molecular weight because the primary flow speed also decreases with molecular weight. As the primary stagnation pressure increases, the bypass ratio decreases, but the compression ratio increases. The net effects of these changes show that the primary stagnation pressure has little effects on I_{sp} except at the very low primary stagnation pressure. At the very low primary stagnation pressure ($p_{tp}/p_0 \leq 5.0$), the compression ratio approaches one and I_{sp} decreases rapidly. The smaller molecular weights produce larger bypass ratios, but this advantage rapidly diminishes as the stagnation pressure increases. These results show that ejector performance does not improve significantly beyond certain primary stagnation pressure.

Figure 2d shows the effects of the primary rocket stagnation pressure and its molecular weight on the thrust augmentation factor and the thrust per unit area of the ejector. The thrust augmentation factor increases with molecular weight. This is because the thrust augmentation factor is inversely proportional to $\sqrt{(R_p)}$. Thus, the thrust augmentation factor is smaller for lower molecular weight in spite of higher bypass ratio and compression ratio. The thrust augmentation factor decreases as the primary pressure increases because of decreasing bypass ratio. At very low stagnation pressure, the thrust augmentation factor decreases rapidly due to lower compression ratio. The thrust increases with molecular weight because of the associated larger primary flow rate, and it increases almost linearly with the stagnation pressure.

In terms of specific impulse, bypass ratio, and thrust augmentation factor, reducing the primary rocket stagnation pressure seems to improve performance. However, total thrust must be considered as well in designing an ejector. Reducing stagnation pressure requires a corresponding increase in ejector area to generate the same amount of thrust. For the given configuration, a hydrogen ejector can be operated at much higher stagnation pressure than a water vapor or hydrocarbon ejector and is capable of producing much higher thrust and specific impulse.

Effects of Primary Flow Stagnation Temperature

The typical results obtained by varying the primary rocket stagnation temperature, T_{tp}/T_0, from 5 to 15, while holding other baseline variables constant ($p_{tp}/p_0 = 15$ and $A/A_p^* = 12$) are discussed hereafter. Again, the ground-level starting condition ($M_0 = 0.01$) is considered.

The primary and secondary flow inlet Mach numbers decrease with increasing stagnation temperature as expected because the increased stagnation temperature decreases the primary flow mass flow rate. The variations of inlet Mach numbers are not shown for the brevity of presentation.

There are limiting stagnation temperature ranges in which the ejector cannot operate effectively because of low compression ratios. The compression ratio p_{te}/p_0 is less than unity when the stagnation temperature is less than 9.0 for $M_{w_p} = 29$ and less than 6.0 for $M_{w_p} = 18$. No temperature limitation is found for $M_{w_p} = 2$. This is due to the relatively high primary flow speed even at these low temperatures.

Figure 3a shows I_{sp} and α variations as functions of primary flow stagnation temperature and molecular weight. The specific impulse increases rapidly as the temperature increases for $M_{w_p} = 2$ and moderately for $M_{w_p} = 18$ and 29. The bypass ratio also increases moderately as the temperature increases for $M_{w_p} = 18$ and 29, but it is relatively insensitive to temperature increase for $M_{w_p} = 2$.

Figure 3b shows the effects of primary flow stagnation temperature on the thrust and the thrust augmentation factor. The primary mass flow rate and the primary flow speed are two competing factors

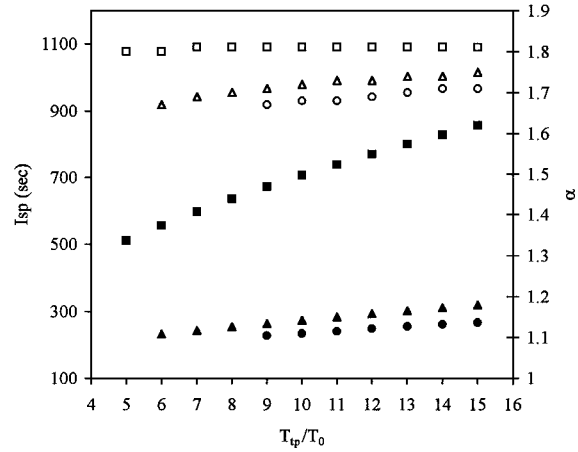

a) Specific impulse and the bypass ratio

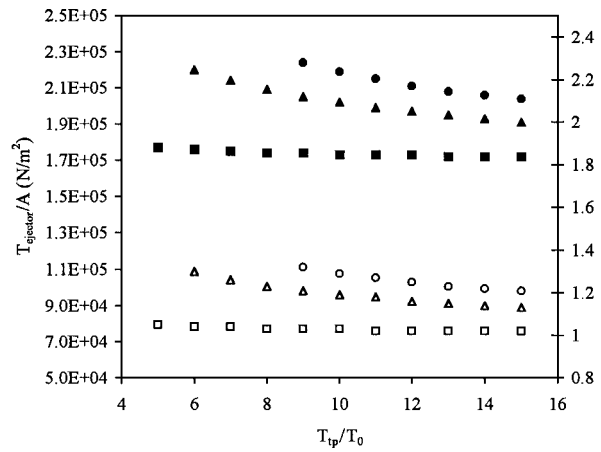

b) Total thrust and the thrust augmentation factor

Fig. 3 Effects of the primary flow stagnation temperature (T_{tp}/T_0) and the molecular weight (M_{w_p}) on the baseline ejector performance at sea level ($M_0 = 0.01$) with $P_{tp}/P_0 = 15$ and A/A_p^*12: $M_{w_p} = 2$ (□), $M_{w_p} = 18$ (△), and $M_{w_p} = 29$ (○). (Open symbols for the left ordinate and filled symbols for the right ordinate.)

that influence the thrust and thrust augmentation. As the stagnation temperature increases, the primary mass flow rate decreases, whereas the primary flow speed increases. Both the thrust and thrust augment factor decrease moderately for $M_{w_p} = 18$ and 29. This implies that the primary mass flow rate has more effect than the primary flow speed when the molecular weight is large. For $M_{w_p} = 2$, decreased primary mass flow rate is balanced by the increased primary flow speed and both thrust and thrust augmentation factor decrease only slightly.

Effects of Ejector Area

The typical results obtained by varying A/A_p^* from 6 to 30, while other variables are fixed at the baseline condition ($p_{tp}/p_0 = 15$ and $T_{tp} = T_0 = 10$), are discussed hereafter.

The inlet Mach numbers decrease rapidly for large molecular weight when the area ration is smaller than 12. The inlet Mach numbers change very little at higher area ratio. For the brevity of presentation, inlet Mach number variations are not shown.

The minimum area ratio required to accommodate primary flow expansion is 8 for $M_{w_p} = 18$ and 10 for $M_{w_p} = 29$. No minimum area ratio is noticed for $M_{w_p} = 2$. This implies that a hydrogen ejector can operate with relatively smaller ejector size.

Figure 4a shows that the specific impulse increases as the area ratio increases for $M_{w_p} = 29$ and for $M_{w_p} = 18$. For $M_{w_p} = 2$, it remains almost constant until $A/A_p^* = 12$ and then increases only slightly as the area ratio increases. The bypass ratio is a very strong function of the area ratio. It increases as the area ratio increases for all molecular weights. The rate of increase grows with decreasing molecular weight.

Figure 4b shows that the thrust augmentation factor generally increases (more rapidly as the molecular weight increases) as the area ratio increases. The thrust per unit area decreases as the area ratio increases for all molecular weights because larger area ratio implies smaller throat area (A = constant) and smaller primary mass flow rate.

The effects of area ratio can be summarized as follows. A large ejector area ratio improves the bypass ratio and the thrust augmentation and slightly increases specific impulse, but decreases thrust per unit ejector area. The effects of area ratio are more significant for larger molecular weights.

Effects of Freestream Conditions

The preceding analysis examined the effects of several ejector variables when the freestream Mach number (M_0) is 0.01, which represents the initial acceleration of the vehicle. To see the effects of primary flow molecular weight in flight conditions, it is assumed that the vehicle flies along a path with constant dynamic pressure of 48 Pa (10^3 lbf/ft^2). The standard atmospheric pressure, and temperature corresponding to the flight path, are then related to the flight Mach number.[11] For the given dynamic pressure, the engine leaves the ground level when the vehicle speed reaches a Mach number of 0.821.

Representative predictions pertinent to the performance of an ejector with the baseline conditions ($p_{tp}\, p_0 = 15$, $T_{tp}/T_0 = 10$, and $A/A_p^* = 12$) are shown in Fig. 5 as M_0 varies from 0.01 to 3.0. Note that the stagnation pressure and temperature ratios are relative to the atmospheric conditions at the altitude corresponding to M_0. Thus, the absolute stagnation pressure and temperature of the primary rocket decrease as the flight speed increases.

Figure 5a shows M_{pi} and M_{si} as a function of M_0 for three primary flows. Note that any inlet shocks for $M_0 > 1$ are neglected, and, thus, $p_{t0} = p_{ts}$. The inlet secondary Mach number changes very little and remains subsonic. However, inlet primary Mach number decreases rapidly as M_0 increases. This is because, as M_0 increases the static pressure at the inlet of the mixing region, p_i/p_0 increases (as shown in Fig. 5b, see following paragraph). The primary Mach number remains supersonic until M_0 reaches about 2.0 for $M_{w_p} = 2$ and about 2.2 for the larger molecular weights. Therefore, ejector mode operations at M_0 greater than 2.0 do not offer performance improvement, and the engine should be switched to the ramjet mode.

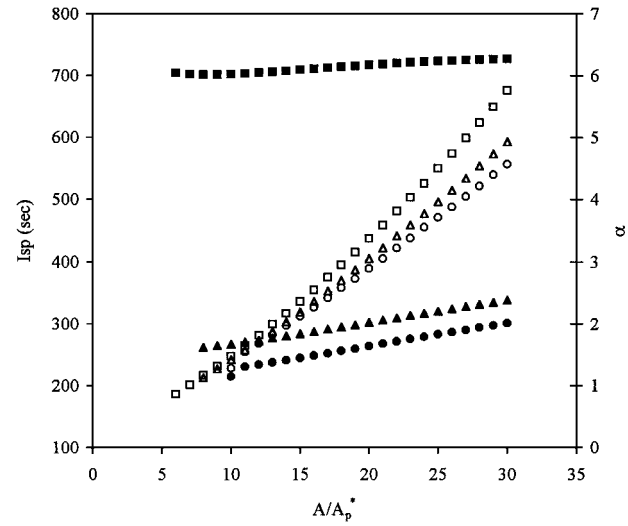

a) Specific impulse and the bypass ratio

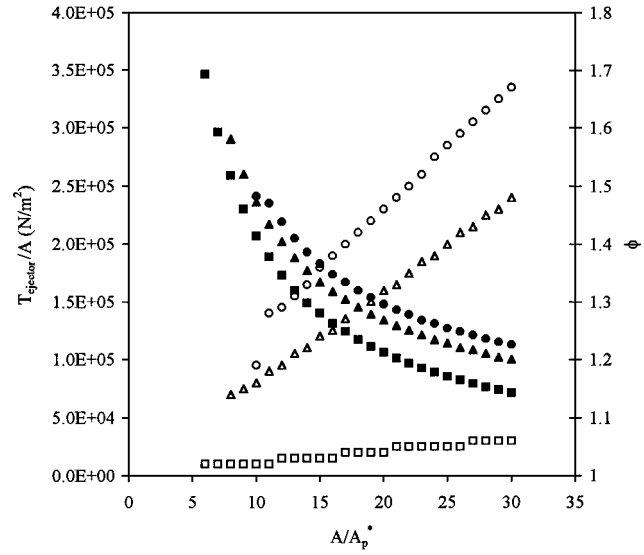

b) Total thrust and the thrust augmentation factor

Fig. 4 Effects of the ratio of ejector area to the rocket throat area (A/A_p^*) and the molecular weight (M_{w_p}) on the baseline ejector performance at sea level ($M_0 = 0.01$) with $P_{tp}/P_0 = 15$ and $T_{tp}/T_0 10$: M_{w_p} = 2 (□), M_{w_p} = 18 (△), and M_{w_p} = 29 (○). (Open symbols for the right ordinate and filled symbols for the left ordinate.)

Figure 5b shows the static pressure at the inlet of the mixing region and the area fraction occupied by the secondary flow A_{si}/A. As the flight speed increases, the stagnation pressure of the atmosphere increases, resulting in the increased static pressure p_i/p_0 at the inlet of the mixing region. The static pressure p_i/p_0 is greater than one except for values of M_0 less than about 0.2. As M_0 increases, the area needed for the secondary flow increases until it reaches a maximum at about $M_0 = 2$. At this point, the primary flow becomes subsonic, as shown in Fig. 5a, and ejector performance becomes poor. Because the primary mass flow rate is smaller for smaller molecular weight, the area occupied by the secondary flow is larger for smaller molecular weight. This is more evident when the vehicle is at sea level ($M_0 < 0.812$).

Figure 5c shows the specific impulse and the bypass ratio as functions of M_0 for the baseline case with three primary fluids. The specific impulse increases with decreasing molecular weight and increasing flight speed for the entire flight speed range. Similar to the specific impulse, the bypass ratio also increases with decreasing molecular weight and increasing flight speed. The sensitivity to the flight speed increases with decreasing molecular weight. The rapid increase in I_{sp} in the supersonic flight regime is due to the increased bypass and compression ratios.

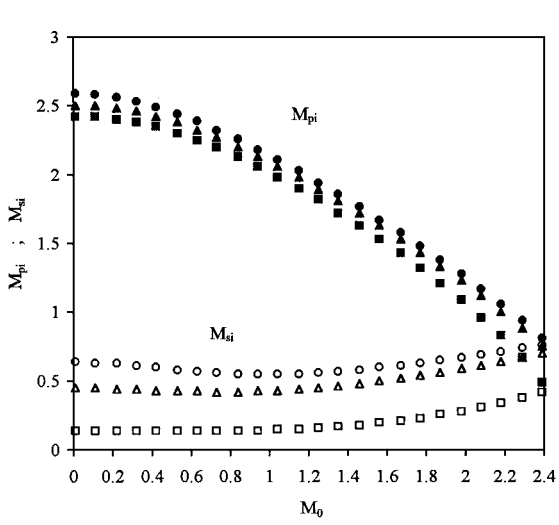

a) Primary and secondary flow inlet Mach numbers

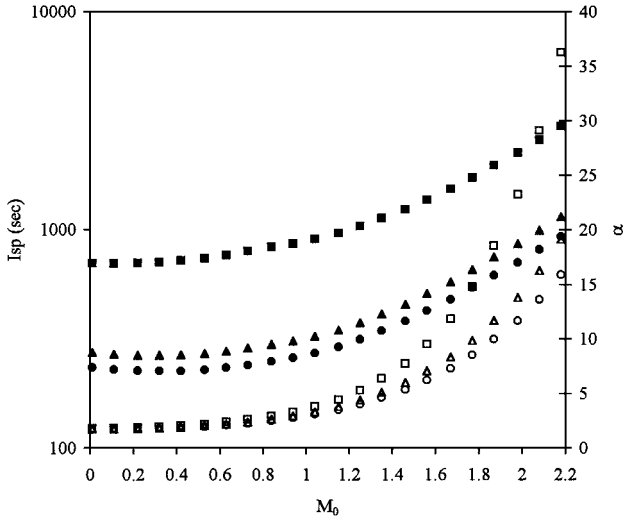

c) Specific impulse and the bypass ratio

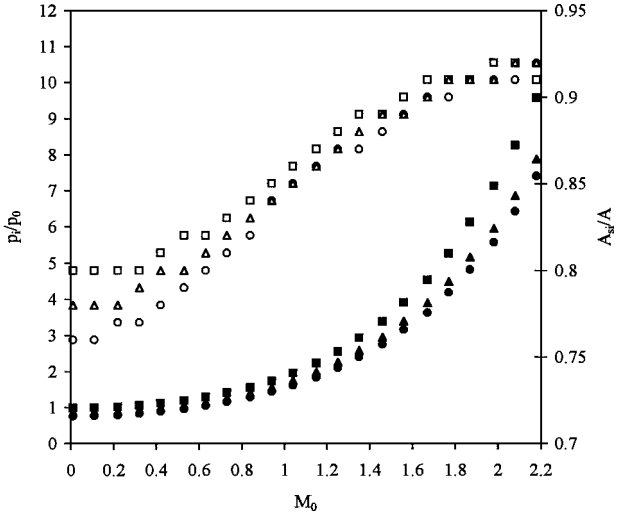

b) Inlet pressure p_i/p_0 and the area ratio A_{si}/A

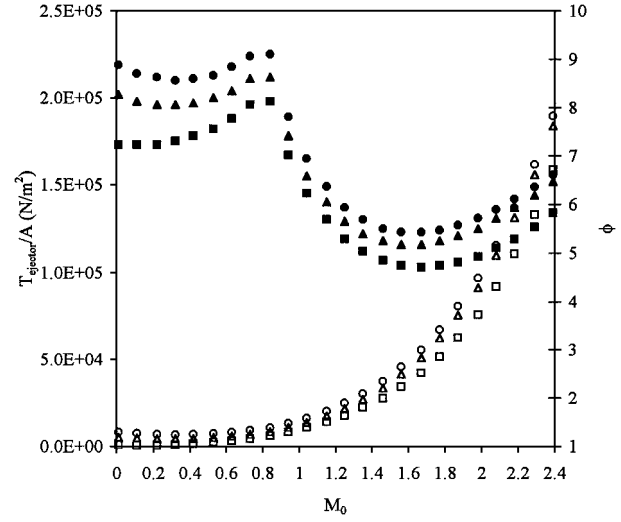

d) Total thrust and the thrust augmentation factor

Fig. 5 Effects of the freestream Mach number (M_0) and the molecular weight (M_{wp}) on the baseline ejector performance with $p_{tp}/p_0 = 15$, $T_{tp}/T_0 = 10$, and $A/A_p^* = 12$: $M_{wp} = 2$ (□), $M_{wp} = 18$ (△), and $M_{wp} = 29$ (○). (Open symbols for the right ordinate and filled symbols for the left ordinate.)

Figure 5d shows the thrust and the thrust augmentation factor. The thrust increases with increasing molecular weight for all flow speeds due to larger mass flow rate and consequently larger combustion energy release. With the selected dynamic pressure of 47 Pa, the vehicle remains on the ground until the flight speed reaches about $M_0 = 0.83$. Thus, the thrust is large in subsonic flight regime. As the vehicle accelerates beyond $M_0 = 0.83$, the thrust first decreases rapidly with increasing vehicle altitude because of exponentially decreasing primary stagnation pressure. It increases again with altitude as the secondary mass flow rate increases with increasing M_0. The thrust augmentation factor is about 1.2–1.5 at the ground level, but it increases rapidly as the flight speed increases. At $M_0 = 2.0$, the thrust augmentation factor is about 5.0 for $M_{wp} = 29$ and about 3.8 with $M_{wp} = 2$. As noted before, the large thrust and thrust augmentation factors for M_0 greater than 2.0 are due to the high compression ratio inherent in the ram mode operation of the airbreathing engine.

Hydrogen Ejector

Low molecular weight primary flow produces higher specific impulse and higher bypass ratio because of higher primary flow speed. The thrust, however, is lower because of lower mass flow rate of the primary flow. To increase the primary mass flow rate, the stagnation pressure must be increased, and the stagnation temperature must be decreased. For low molecular weight, the stagnation pressure can be increased without difficulty as shown in Fig. 2. Likewise, a low stagnation temperature can be used as shown in Fig. 3. A hydrogen ejector ($M_{wp} = 2$) with $p_{tp}/p_0 = 30$ and $T_{tp}/T_0 = 7$ is considered to compare its performance with the baseline cases with $M_{wp} = 2$ and 29 as a function of flight speed. This combination of high stagnation pressure and low stagnation temperature is not possible for the higher molecular weights. It was found in the present work that there are no solutions with the given stagnation conditions with $M_{wp} = 18$ and 29 at low flight speeds.

Figure 6a shows that the increased stagnation pressure and decreased stagnation temperature reduce the specific impulse and the bypass ratio of the hydrogen ejector. The specific impulse is still much higher than the baseline case with $M_{wp} = 29$ for all flight speeds. Figure 6b shows the thrust and thrust augmentation factor of this modified hydrogen ejector in comparison with other baseline ejectors. Because of the increased mass flow rate, a dramatic increase in the thrust is seen over the entire range of flight speeds. The increased thrust is much higher than the baseline case with $M_{wp} = 29$ with the same ejector area ratio. It may be concluded that the ejector size can be made much smaller for a hydrogen ejector with appropriate stagnation conditions (higher p_{tp}, lower T_{tp}) while producing the same amount of thrust with much higher specific impulse than ejectors with higher molecular weight. This is in agreement with a numerical result presented in Ref. 15.

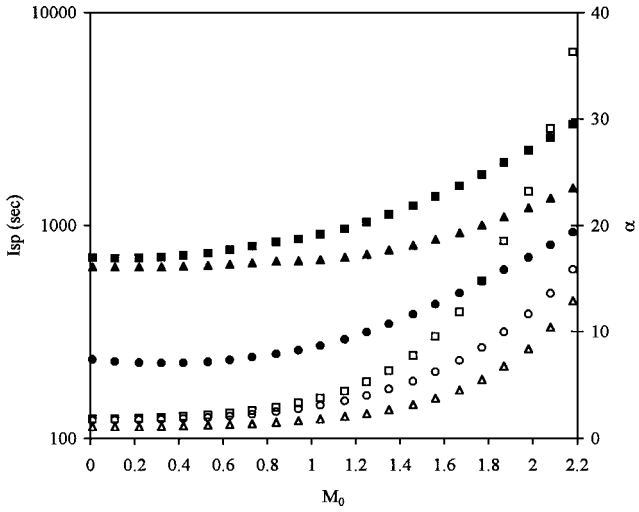

a) Specific impulse and the bypass ratio

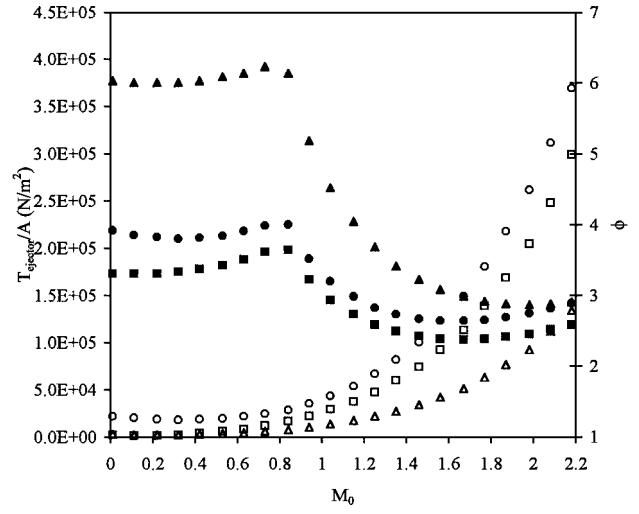

b) Total thrust and the thrust augmentation factor

Fig. 6 Performance comparison of a modified hydrogen ejector along a flight path with two baseline ejectors; the modified hydrogen ejector has a higher primary flow stagnation pressure ($p_{tp}/p_0 = 30$) and a lower primary flow stagnation temperature ($T_{tp}/T_0 = 7$) than the baseline ejector ($p_{tp}/p_0 = 15, T_{tp}/T_0 = 10$, and $A/A_p^* = 12$). The ejector area ratio remains constant ($A/A_p^* = 12$): baseline hydrogen ejector (□), baseline hydrocarbon ejector (○), and modified hydrogen ejector (△). (Open symbols for the right ordinate and filled symbols for the left ordinate.)

Conclusions

The effects of the molecular weight of the gas used by the primary rocket of a generic ejector–ram rocket RBCC engine were investigated by using steady-state one-dimensional compressible flow equations. Three primary gases with the molecular weights of 2, 18, and 29 were analyzed, covering a wide range of operating conditions in terms of primary rocket stagnation conditions, ejector geometry, and freestream velocity.

The specific impulse and the bypass ratio increase with decreasing molecular weight. The specific impulse increases slightly with increasing primary stagnation pressure for $M_{w_p} = 2$, but it decreases slightly for larger molecular weights. The specific impulse increases with increasing stagnation temperature and increasing ejector area. The bypass ratio decreases rapidly as the primary rocket stagnation pressure increases, but it increases with increasing stagnation temperature and increasing ejector area.

The thrust and the thrust augmentation factor, on the other hand, increase with increasing molecular weight. The thrust increases almost linearly with stagnation pressure but decreases as the stagnation temperature and the ejector area increase. The thrust augmentation factor decreases as the stagnation temperature and pressure increase and increases as the ejector area increases.

Effects of the freestream conditions on the ejector efficiency are significant for all molecular weights. The inlet pressure p_i/p_0 increases as the freestream velocity increases. Consequently, the primary flow inlet Mach number decreases continually and finally becomes subsonic at about $M_0 = 2$. Therefore, ejector performance becomes poor at flight speeds higher than about $M_0 = 2$ for all molecular weights.

There are limitations on the allowable maximum primary rocket pressure, minimum primary rocket temperature, and minimum ejector area, which become severe as the molecular weight increases. A hydrogen ejector with high stagnation pressure and low stagnation temperature seems to produce relatively high thrust as well as high specific impulse for all flight speeds.

Acknowledgments

This work was supported by a grant from the Advanced Space Transportation Program, NASA Marshall Space Flight Center, NAG8-1794. The authors are grateful to John Hutt (Program Manager) and John Blevins (Contract Officer's Technical Representative) for their guidance and support and to Uwe Heuter and John Cole for their encouragement. S. Han expresses his appreciation to Don Bai and Charles Schafer for stimulating discussions on the rocket-based combined-cycle engine concepts. The authors also express sincere gratitude to one of reviewers for constructive criticism.

References

[1]Hueter, U., "Advanced Reusable Transportation Technologies Project Overview," AIAA Paper 96-4603, Nov. 1996.

[2]Escher, W. J. D., and Schnurstein, R. E., "Retrospective on Early Cryogenic Primary Rocket-Based Combined-Cycle Engines," AIAA Paper 93-1944, June 1993.

[3]Dijkstra, F., and Maree, A. G. M., "Experimental Investigation of the Thrust Enhancement Potential of Ejector Rockets," AIAA Paper 97-2756, July 1997.

[4]Fabri, J., and Siestrunck, R., "Supersonic Air Ejectors," *Advances in Applied Mechanics*, Vol. 5, 1958, pp. 1–34.

[5]Emmauel, G., "Optimum Performance for a Single-Stage Gaseous Ejector," *AIAA Journal*, Vol. 14, No. 9, 1976, pp. 1292–1296.

[6]Dutton, J. C., Mikkelson, C. D., and Addy, A. L., "Theoretical and Experimental Investigation of the Constant Area, Supersonic–Supersonic Ejector," *AIAA Journal*, Vol. 20, No. 10, 1982, pp. 1392–1400.

[7]Nagaraja, K. S., and Hammond, D. L., "One-Dimensional Compressible Ejector Flows," AIAA Paper 73-1184, Nov. 1973.

[8]Tillman, T. G., Patterson, R. W., and Presz, W. M., Jr., "Supersonic Nozzle Mixer Ejector," *Journal of Propulsion and Power*, Vol. 8, No. 2, 1992, pp. 513–519.

[9]Work, L. T., and Haedrich, V. W., "Performance of Ejector as a Function of the Molecular Weights of Vapors" *Industrial and Engineering Chemistry*, Vol. 31, No. 4, 1939, pp. 464–477.

[10]Peterson, E. L., Roan, V. P., and Pfahler, J. N., "Experimental Investigation of Supersonic-Primary Dissimilar-Fluid Ejectors," AIAA Paper 92-3793, July 1992.

[11]Heiser, W. H., and Pratt, D. T., *Hypersonic Airbreathing Propulsion*, edited by J. S. Przemieniecki, AIAA Education Series, AIAA, Washington, DC, 1994, pp. 446–452.

[12]Waltrup, P. J., and Billig, F. S., "Structure of Shock Waves in Cylindrical Ducts," *AIAA Journal*, Vol. 11, No. 10, 1973, pp.1404–1408.

[13]Lin, P., Rao, G. V. R., and O'Connor, G. M., "Numerical Investigation on Shock Wave/Boundary-Layer Interactions in a Constant Area Diffuser at Mach 3," AIAA Paper 91-1766, May 1991.

[14]Dutton, J. C., and Carrol, B. F., "Limitation of Ejector Performance Due to Exit Choking," *Journal of Fluid Engineering*, Vol. 110, 1988, pp. 91–93.

[15]Han, S., Bai, D., and Schmidt, G., "Atomic-Based Combined-Cycle Analysis," AIAA Paper 2000-3861, July 2000.